

Wave Chaos in Elastodynamic Cavity Scattering

Andreas Wirzba¹, Niels Sndergaard², and Predrag Cvitanovic³¹ Institut für Kernphysik (Theorie), Forschungszentrum Jülich GmbH, D-52425 Jülich, Germany² Department of Physics & Astronomy, Northwestern University, Evanston, IL 60208-3112³ Center for Nonlinear Science, School of Physics,

Georgia Institute of Technology, Atlanta, GA 30332-0430

(Dated: September 10, 2019)

Exact scattering resonances are calculated for a system of several cylindrical cavities in elastodynamics. In the high frequency limit both classical and complex periodic orbits contribute, with each complex orbit composed of sequences of classical particle trajectory segments with varying polarizations interspersed with surface wave segments. The shortest of these orbits suffice to interpret exact elastodynamic scattering resonances and Wigner time delays.

PACS numbers: 05.45.Mt, 03.65.Sq, 46.40.-f, 46.40.Cd, 46.40.Ff, 62.30.+d

The Gutzwiller semiclassical quantization of classically chaotic systems relates quantum observables such as spectral densities to sums over classical unstable periodic orbits [1, 2]. The work presented here is a step towards a formulation of such approximate short-wavelength theory of wave chaos for the case of linear elastodynamics. Why elastodynamics? The elastodynamics experiments initiated by Oxborrow et al. [3] attain Q values as high as $5 \cdot 10^6$, making spectral measurements in elastodynamics competitive with measurements in microwave cavities at liquid helium temperatures [4], and vastly superior to nuclear physics and room temperature microwave experiments for which the Q values are orders of magnitude lower, typically 10^2 – 10^3 . Elastodynamic experiments are also more flexible and much cheaper than the competitors in atomic physics, helium-cooled microwave cavities or solid state nano-devices.

So far, for elastodynamics we have neither an experimental demonstration of existence of unstable periodic orbits nor a theory that would predict them. While Oxborrow et al. measure accurately half a million spectral lines, the current theory is barely adequate for computation of dozens of resonances. This unsatisfactory state of affairs is the *raison d'être* for the theoretical effort undertaken here.

While current experiments excel in measurements of eigenspectra of compact resonators, the periodic orbit theory computations of such bound system spectra are rendered difficult by presence of non-hyperbolic phase space regions. As our primary goal is to derive and test rules for replacing wave mechanics by the high-frequency ray-dynamic trajectories, we concentrate here instead on the problem of scattering of cylindrical cavities, for which the classical dynamics is fully under control.

In the case of one cavity the exact scattering spectrum is known [5]. For the multiple cavities case we generalize here the S -matrix formalism developed for the quantum-mechanical n -disk scattering [6, 7, 8, 9], and compute the exact resonances and the Wigner time delays from the full elastodynamic wave-mechanical scattering matrix. We

then compare the exact results with the corresponding quantities calculated in the short-wavelength approximation, and discover that the quantum-mechanical intuition fails us: the Rayleigh surface waves (which have no analog in the quantum scattering problem) dominate the spectrum, rendering even a two-disk elastodynamic scattering problem chaotic.

Elastodynamics. Consider an infinite slab of an isotropic and homogeneous elastic material (e.g., polyethylene or isotropic quartz) with parallel top and bottom plane boundaries, and an in-phase stimulus such that the system behaves quasi-two-dimensionally along the slab, with no excitation of or coupling to waves propagating perpendicular to the slab.

The propagating waves are either the pressure or the shear solutions of the Navier-Cauchy equation [10]

$$\nabla^2 u + (\lambda + \mu)^{-1} \nabla(\nabla \cdot u) - \rho^{-1} \omega^2 u = 0;$$

where $u(r)$ is a vectorial displacement field, and λ and μ are the Lamé constants, ρ the mass density and ω the frequency. The experiments dictate free boundary conditions, with vanishing traction [10]

$$t(u) = \sigma_{ij} n_j = 0 \quad (1)$$

Here \hat{n} is a unit vector normal to the boundary, $\mathbb{1}$ the unit matrix, and T indicates a transposition.

Compared to quantum mechanics (QM), elastodynamics offers new and interesting challenges: Elastodynamic waves are vectorial, with the pressure wave propagating through the bulk with velocity $c_p = \sqrt{(\lambda + 2\mu)/\rho}$, and the shear wave with velocity $c_s = \sqrt{\mu/\rho}$. Furthermore, the Rayleigh surface waves propagate along plane boundaries with no attenuation, and velocity c_R determined [5, 10] by the condition $c_R^3 = c_s^3 + c_p^3$,

$$0 = 2^2 c_R^3 - 3 c_s^2 c_R - c_p^2 c_R^3 \quad (2)$$

When either a shear or pressure plane wave hits a boundary, mode conversion can take place [11], with two or

more plane waves emitted at different angles, as well as the surface Rayleigh waves which can travel along curved boundaries with very little attenuation. They, as we shall see, will require inclusion of complex periodic orbits into the short-wavelength theory, rendering the elastodynamic wave chaos radically different from that encountered in the semiclassical theory of quantum systems.

We now drill one, two, or more cylindrical cavities perpendicularly through the slab. For concreteness, in all numerical calculations reported here we take the medium to be polyethylene (which has a bad Q -value of 10^2 , but which is used in Ref. [5]) with $c_L = 1950$ m/s, $c_T = 540$ m/s, and $c_R = 513$ m/s.

One-cavity scattering. In the case of one cavity the exact scattering spectrum is known [5]. Just as for the one-disk scattering matrix [9, 12] of quantum mechanics, $S_{mm^0}^{(1)} = t_{m^0}^{(+)}(ka) H_m^{(+)}(ka)$, $m; m^0 = 0; 1; 2; \dots$; the scattering of a single cylindrical cavity is separable in angular momentum. The one-cavity S -matrix of elastodynamics, a $[2 \times 2]$ matrix in $fL; Tg$ components, is determined by the traction matrices

$$S_{mm^0}^{(1)} = t_{m^0}^{(+)}(a)^{-1} t_m^{(+)}(a) : \quad (2)$$

The traction matrices of angular momentum m , polarization $2fL; Tg$ and spatial index $i2ff; \hat{g}$ result when outgoing (+), incoming (−) or regular (J) radial displacements are inserted into the formula (1) for the traction. They can be expressed in terms of Hankel (Bessel) functions and their derivatives

$$\frac{a^2}{2} t_m^{(+)}(a)_i = \lim_{k \rightarrow 0} (1 - i) k^2 \frac{d}{dk} \frac{H_m^{(+)}(ak)}{k} + (1 - i) k \frac{d}{dk} \left[m^2 - \frac{1}{2} k_T^2 a^2 \right] H_m^{(+)}(ak) :$$

The scattering resonances for the one-cavity elastodynamic medium with traction-free boundary conditions are then determined [5] from $\text{Det } t_m^{(+)}(a) = 0$.

In the one-cavity case a sophisticated theory of ray dynamics already exists. The main tool is the Sommerfeld-Watson transformation which in the QM case replaces a slowly converging partial wave sum by a fast converging sum over complex creeping trajectories, first derived by Franz [12]. Similar calculations have been carried in elastodynamics [13]. The pressure and shear Franz resonances also exist here, but for elastodynamics the one-cavity spectrum is dominated by the weakly damped Rayleigh resonances, with no QM counterpart.

Just like the Franz resonances, the Rayleigh resonances ! are determined via the complex angular momenta $R(!)$ by the resonance condition $1 - \exp i2R(!) = 0$.

In the spirit of Keller's geometrical theory of diffraction [13] we now use this exact wave-mechanical result to assign a ray-dynamic weight to a segment of the boundary traversed by a Rayleigh wave. A circular

Rayleigh segment of arc length a is given the complex-valued weight $\exp(i2R(!))$, such that the effective path length of a Rayleigh segment is $R(!) = k_T a$.

The short-wavelength approximation to the resonance condition produces an analytical expression only for the real part of $R(k)$. As the imaginary term is nonvanishing and important for the strengths of the resonances, we take the exact wave-mechanical $R(!)$, determined by $\text{Det } t_{R(!)}^{(+)}(a) = 0$ as the definition of the complex Rayleigh trajectory segment.

Multi-cavity scattering, exact spectrum. Following the QM methods of Refs. [7, 8, 9], we decompose the S -matrix for the n -cavity system as

$$S_{mm^0}(!) = 1_{mm^0} + i \sum_{j; j^0=1}^{X^n} C_{m1}^j M_{11^0}^{-1} D_{11^0}^{jj^0} D_{Tm^0}^{j^0}$$

where $C_{m1}^j, M_{11^0}^{jj^0}$, and $D_{11^0}^{jj^0}$ are $[2 \times 2]$ matrices in the wave polarization space $fL; Tg$; $0; 0$, and $1; 1^0; m^0 = 0; 1; 2; \dots$ are angular momenta. The D matrix translates the initial scattering wave ($m; j$) from the global coordinate system to the one of cavity j^0 and couples there the initial wave to the internal wave ($l^0; 0$). The C matrix couples the internal wave ($l; j$) to the outgoing scattering wave ($m; j$). The matrix M , the inverse of the multi-scattering matrix, can be written as $1 + A$ where the matrix A evolves the internal wave from the cavity j^0 , polarization ($l^0; 0$) to the cavity j , polarization ($l; j$):

$$A_{11^0}^{jj^0} = (1 - i) \frac{a_j}{a_{j^0}} t_1^{(j)}(a_j) T_{11^0}^{(+); jj^0} t_p^{(+)}(a_{j^0})^{-1} ; h T_{11^0}^{(+); jj^0} = H_{11^0}^{(+)}(k R_{jj^0}) e^{i l j^0} i l^0 (j^0) :$$

$T^{(+); jj^0}$ is the translation matrix from the coordinate system with origin at the center of cavity j^0 to the one based at the cavity j , and R_{jj^0} and j^0 are the relative center-to-center distances and angles [9, 14]. The factor $(1 - i)_{jj^0}$ ensures that successive cavities visited by the wave differ.

The determinant of the S -matrix contains all spectral information. As in the QM, it factorizes [9, 14]:

$$\det S(!) = \prod_{j=1}^8 \det S_j^{(1)}(!) \frac{D \det M(!)^9}{D \det M(!)} : \quad (3)$$

The genuine multi-scattering scattering resonances are given by the zeros of $D \det M(!)$, and the cluster phase shift is defined as $\phi_{c1}(!) = \frac{1}{i} \ln D \det M(!)^9 = D \det M(!)$. In QM the Gutzwiller-Voros Zeta function is the semiclassical approximation to $D \det M$, where the connection follows via the semiclassical reduction of the traces $\text{Tr}(A^N)$ appearing in the cumulant expansion

$$D \det M(k) = 1 + \text{Tr} A - \frac{1}{2} \text{Tr} A^2 + (\text{Tr} A)^2 + \dots :$$

As shown in Ref. [9], in the short wavelength approximation the traces $\text{Tr} A^N$ reduce to the set of ray-dynamic

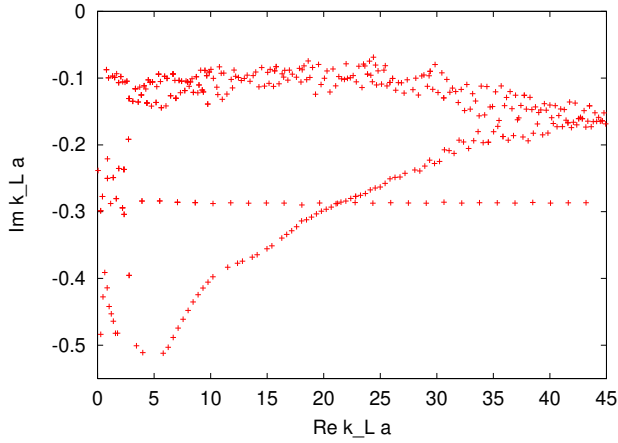


FIG. 1: A_1 resonances of elastodynamic two-cavity system with traction-free boundaries, in the complex pressure wave number plane $k_L = \omega/c_L$.

periodic orbits of topological length n , whereas the cumulants become "curvatures" (periodic orbits shadowed by pseudo orbits [2]).

Here we present a few typical numerical results for the A_1 subspace of the system of two cylindrical cavities of radius $a = 1$ cm, and center-to-center separation $R = 6$ cm (the full results are given in Refs. [14, 15]). The two-fold reflection symmetry implies that the determinant factors into the four irreducible representations; the fully symmetric A_1 , the fully antisymmetric A_2 , and two mixed symmetry representations B_1 and B_2 of the C_{2v} discrete symmetry group [7, 8, 9]. The transfer matrix for each irreducible subspace is defined on the fundamental domain, a quarter slab whose 4 copies tile the whole elastodynamic slab. The A_1 resonances determined by the zeros of $\text{Det}(1 + A_{A_1})$ are shown in Fig. 1.

Multi-cavity scattering, ray-dynamic interpretation. The shortest periodic orbits in the fundamental domain are of topological length one and are derived from the short-wavelength approximation to $\text{Tr}A_{A_1}$. Following the methods of Refs. [8, 9] we can immediately extract the weights $t_{\text{pr}}; t_{\text{tr}}$ of the classical orbits bouncing between the two cavities which, in the A_1 representation, are of form $t = \frac{\exp(ik_L(R-2a))}{p}$ with $p = \frac{1}{R-a} + \frac{1}{R+2a}$. Furthermore, two complex periodic orbits that have the form of an oval and figure eight [8] contribute. Their Rayleigh wave segments are weighted by $\exp(i\alpha_R)$, determined above, and connected to the geometrical segments of orbits by the diffraction constants determined by Keller and Karal [13]. At the second trace level, in addition to the expected geometrical and repeated orbits two new Rayleigh-type orbits appear, and so on for longer periodic orbits, see Fig. 2. In Fig. 3 we plot the exact Wigner time delay $\frac{d}{dk_L} \text{cl}$ of the cluster phase shift as function of the pressure wave number k_L , and compare it

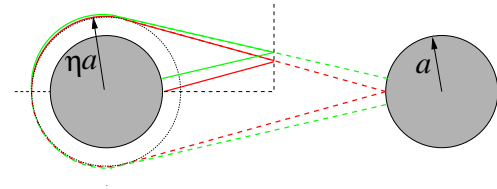


FIG. 2: Two periodic orbits of Rayleigh-type and topological length 2 that have no counterpart at lower order, plotted also in the fundamental domain of the two-cavity system.

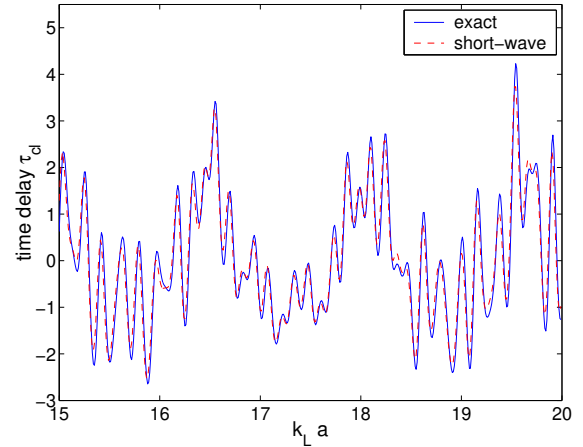


FIG. 3: Wigner time delay for the two-cavity system, the exact vs. the ray-dynamic expansions, as function of the pressure wave number k_L .

to the short-wavelength curvature expansion based on the geometrical and complex periodic orbits described above. The short-wavelength periodic orbit approximation is in good agreement with the exact cumulant expansion to second order. Finally, in Fig. 4 we compare the moduli of the Fourier transformations of $\text{Tr}A_{A_1}$ and $\text{Tr}A_{A_1}^2$ for the region $10 < k_L a < 45$ with the corresponding transformation of the sum of all periodic orbits of topological length one and two, respectively. This is done in order to compare the periods of the ray-dynamic prime periodic orbits with the Fourier peaks of the exact wave-mechanical data. The time values of the Fourier peaks indeed correspond to the periodic orbit periods $T = \frac{l_{\text{pr}}}{c_L} + \frac{l_{\text{tr}}}{c_T} + \frac{l_{\text{pr}}}{c_L} + \frac{l_{\text{tr}}}{c_T} + \frac{l_{\text{pr}}}{c_L} + \frac{l_{\text{tr}}}{c_T}$ with $l_{\text{pr}}, l_{\text{tr}}$ and a_{pr} the geometrical lengths of the pressure, shear and Rayleigh segments, respectively. A gain, the short-wave approximation captures nearly all qualitative features of the exact calculation. However, the $1/k_L$ corrections are still not negligible, as can be seen from the small structure close to 0.1 ms in Fig. 4 (b) that corresponds to a combined LT geometric orbit. Such orbit vanishes in the short-wavelength approximation, as there is no coupling of pressure to shear rays at perpendicular impact. The contributing complex orbits visible in Fig. 4 have only shear segments coupled to Rayleigh

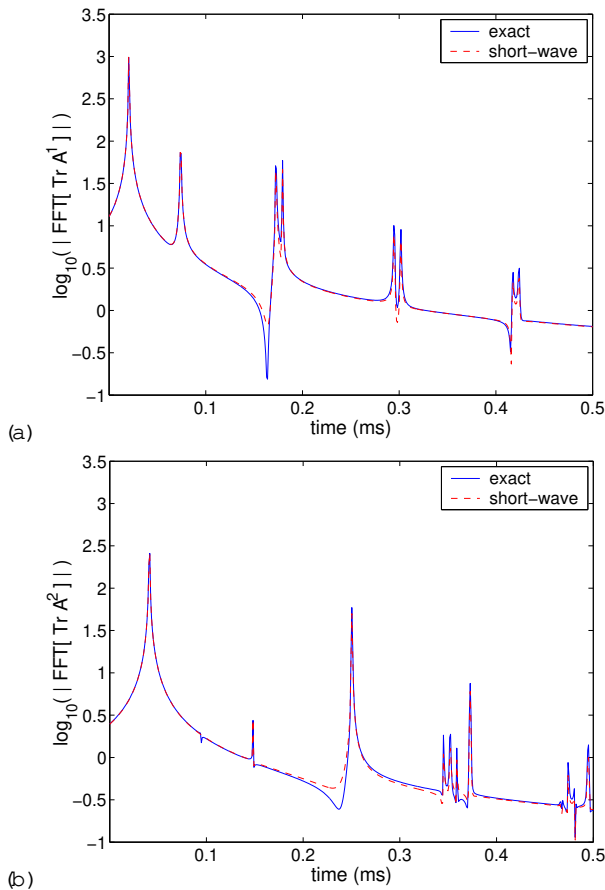


FIG. 4: Comparison of the Fourier transformations of the exact traces $\text{Tr}A_{A_1}$, $\text{Tr}A_{A_1}^2$ of the two-cavity system with the short-wavelength approximation based on (a) periodic orbits of topological length one, (b) periodic orbits of topological length two, in the range $10 < k_L a < 45$. All peaks are identifiable as the periods of the shortest period orbits.

segments (since $c_T < c_R$), whereas the coupling of pressure segments to Rayleigh segments is so severely suppressed that there is no trace of them detectable in the Fourier transforms. This explains all qualitative features of Fig.4. The regular band of subleading resonances in Fig.1 at $\text{Im } k_L = 0.29\pi a$ is nothing but the resonances of the t_L orbit that dominates the QM case. However, for the elastodynamics this is an exponentially small effect: the chaotic band of the leading resonances results from the interference of the t_T orbit and the exponentially growing number of Rayleigh orbits. For the k_L window shown in Fig.1, the periodic orbit sum can be truncated at length four, since the spectrum generated from the cumulant expansion to fourth order does not differ from the full one to the printer resolution.

Summary and outlook. We have derived the scattering determinant and determined the exact scattering resonances and Wigner time delays for a quasi-two-dimensional isotropic and homogeneous elastodynamic

slab with several cylindrical cavities.

To the second order in the cumulant expansion the short-wavelength ray-dynamics estimates and the exact Wigner time delays for the two-cavity system are in good agreement. The two-cavity scattering system clearly demonstrates that surface orbits of Rayleigh type dominate the leading part of the spectrum. They have no counterpart in quantum mechanics. In particular, the elastodynamic resonance spectrum for two-cavities scatterer is dominated by an infinite number of weakly attenuated complex periodic orbits of Rayleigh type, and is in that sense chaotic, contrary to the QM case.

In contrast to the creeping rays in the QM case [16], so far we do not have a method to compute contributions of Rayleigh-type rays for arbitrary curved billiard boundaries, and extend the high-frequency approximation to lower frequencies. As long as this is so, we cannot state the full Gutzwiller-Voros type Zeta function for the elastodynamic case. Generalizations to anisotropic media (the highest Q-value experiments are performed on single crystals of quartz), and applications of the above ray-dynamics techniques to resonator geometries used in experiments remain open problems.

- Current address: Theoretical Mechanics Department, University of Nottingham, Nottingham NG7 2RD, UK
- [1] M.C. Gutzwiller, *Chaos in Classical and Quantum Mechanics* (Springer, New York, 1990).
 - [2] P. Cvitanovic et al., *Classical and Quantum Chaos*, www.nbi.dk/ChaosBook/ (Niels Bohr Institute, Copenhagen, 2001).
 - [3] C. Eilegaard, T. Guhr, K. Lindemann, J. Nygaard and M. Oxborrow, *Phys. Rev. Lett.* **77**, 4918 (1996).
 - [4] H.D. Graf et al., *Phys. Rev. Lett.* **69**, 1296 (1992); H. Ait et al., *Phys. Rev. Lett.* **74**, 62, (1995).
 - [5] J.L. Izbicki et al., *Wave Motion* **28**, 227 (1998).
 - [6] M.V. Berry, *Ann. Phys. (N.Y.)* **131**, 163 (1981).
 - [7] P. Gaspard and S.A. Rice, *J. Chem. Phys.* **90**, 2225 (1989); **90**, 2242 (1989); **90**, 2255 (1989).
 - [8] A. Wirzba, *CHAOS* **2**, 77 (1992); *Nucl. Phys. A* **560**, 136 (1993).
 - [9] A. Wirzba, *Phys. Rep.* **309**, 1 (1999).
 - [10] L.D. Landau and E.M. Lifshitz, *Theory of Elasticity* (Pergamon, Oxford, 1959).
 - [11] L. Couchman et al., *Phys. Rev. A* **46**, 6193 (1992).
 - [12] W. Franz, *Z. Naturforschung* **9a**, 705 (1954).
 - [13] J.B. Keller and F.C. Karal, Jr., *J. Acoust. Soc. Am.* **36**, 32 (1964).
 - [14] N. Sndergaard, *Wave Chaos in Elastodynamic Scattering*, PhD thesis (Northwestern University, Evanston, 2000); www.nbi.dk/nsnderg.
 - [15] N. Sndergaard et al., (in preparation).
 - [16] G. Vattay et al., *Phys. Rev. Lett.* **73**, 2304 (1994); P.E. Rosenqvist et al., *J. Stat. Phys.* **83**, 243 (1996).